Emission spectra of electron-hole drops in gallium phosphide

N. R. Nurtdinov and A. É. Yunovich

Moscow State University

(Submitted 12 April 1982)
Zh. Eksp. Teor. Fiz. **83**, 1870–1878 (November 1982)

The photoluminescence spectra of epitaxial GaP layers with impurity density $\lesssim 10^{16}$ cm^{-3} are investigated at $T = 8$–60 K. Emission due to electron-hole drops (EHD) is observed at excitation levels $W = 3\times10^3$–2×10^5 W/cm^2. The shape of the EHD spectral band with a maximum at $\hbar\omega_m = 2.268$ eV is independent of W and T at $T \lesssim 40$ K, and the band has characteristic recombination times 30 ± 3 nsec and a critical temperature $T_c = 50^{+5}_{-3}$ K. The shape of the EHD spectrum is analyzed with account taken of the two-hump structure of the conduction band and of the different ratios of the probabilities of emission of *TO*, *LA*, and *TA* phonons in indirect transitions. The obtained values of the Fermi levels, of the carrier-pair densities in the EHD, and of the binding energy require corrections necessitated by allowance for the phonon dispersion and carrier heating in the EHD. The recombination band assumed to be due to a low-density electron-hole plasma is found to be significant in the quantum-energy region ~ 2.29 eV near the short-wave edge of the EHD band at high T.

PACS numbers: 78.55.Ds, 71.35. + z

1. INTRODUCTION

Investigations of electron-hole drops (EHD) in Ge and Si (see the reviews[1–3]) and of radiative recombination in GaP (see the reviews[4,5]) have led recently to observation of EHD in GaP (Refs. 6–9) and to an understanding of the singularities of their emission spectra.[10,11] The conduction band of GaP has a complicated two-hump structure[12–14] whose parameters were determined quite accurately in Refs. 14–16; this structure must be taken into account in the analysis of properties of EHD.[9–11] It was predicted back in Ref. 5 that EHD in GaP are possible at relatively high temperatures; experiments[6–11] point for EHD in GaP to critical temperatures that vary in the range $T_c = 30$–70 K. To observe the EHD it is necessary to have GaP crystals with residual-impurity densities $\lesssim 10^{16}$ cm^{-3}; this can be reached by growing the GaP by the liquid-epitaxy method.[17,18]

We report here investigations of the photoluminescence spectra of GaP in a wide range of excitation levels, with variation of the delay time relative to the excitation and temperature. Selection of the purest samples made it possible to identify the emission spectra of the EHD. The shapes of the EHD spectra are calculated with allowance for the latest data on the GaP band structure, which influence the accuracy of the EHD parameters by comparison with experiment.

2. EXPERIMENTAL PROCEDURE AND INVESTIGATED SAMPLES

The luminescence was excited with an LGI-21 nitrogen laser (power density up to $W \lesssim 10^6$ W/cm^2, $\lambda = 337.1$ nm, pulse duration ~ 10 nsec, repetition frequency ~ 100 Hz). The value of W was varied by focussing the spot ($\gtrsim 150$-μm diam) and using filters calibrated accurate to $\pm 15\%$. The spectra were investigated with a high-transmission MDR-1 monochromator (characteristic resolution ~ 0.1 nm) with an FEU-79 photomultiplier (time resolution ≈ 10 nsec). To register the spectra with a time delay we used an S7-8 stroboscopic oscilloscope with the analog signal fed to a KSP-4 or PDS-21 recorder.

The samples were soldered with indium to a copper substrate on the tail of a vacuum helium cryostat. The substrate temperature T was either fixed (8 K) or varied in the range 30–100 K accurate to ± 1 K. The difference between the sample and substrate temperatures determined from the luminescence line shift of an exciton bound to a neutral donor S did not exceed 3–5 K at $W \leqslant 4\times10^5$ W/cm^2.

The GaP samples for the investigations were kindly supplied by O. B. Nevskiĭ; they were grown by liquid-phase epitaxy using vacuum cleaning of the material to rid it of uncontrollable impurities.[17,18] The equilibrium energy density on the surface of the epitaxial layer, according to data on the capacitance of the Schottky barrier at low temperature, was $n < 10^{17}$ cm^{-3}. The samples with the lowest impurity density were selected in accord with their luminescence spectra from a batch of 40 samples, some of which were investigated by layer-by-layer etching.

3. RESULTS OF EXPERIMENTS

3.1. At low excitation density, $W/W_{cr} = 3\times10^3$ W/cm^2, the predominant line in the photoluminescence (PL) spectra at low temperatures was that of an excitation bound on S, $\hbar\omega_m = 2.309 \pm 0.001$ eV at 8 K (see Fig. 1a). Near this line, at lower energy, a shoulder could be distinguished and was ascribed to the line due to recombination of the free exciton with emission of an LA phonon (*X–LA*), $\hbar\omega_m = 2.300 \pm 0.002$ eV.

At excitation densities higher than critical, $W > W_{cr}$, a broad band appears in the spectrum, with a maximum near 2.27 eV, and corresponds to the EHD emission. At $T = 8$ K the spectral position of the maximum was $\hbar\omega_m$(EHD) $= 2.268 \pm 0.001$ eV when W was varied within two orders of magnitude up to $\sim 2\times10^5$ W/cm^3. In this case the shape of the band in the long-wave part and in the region

 0038-5646/82/111080-06$04.00

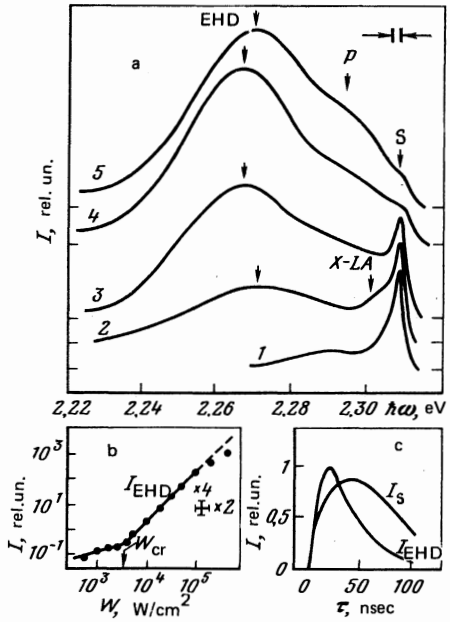

FIG. 1. a) Photoluminescence spectra of GaP sample at $T = 8$ K with increasing excitation level W: $1 - 10^3$, $2 - 2{,}5\times10^3$; $3 - 5\times10^3$; $4 - 2\times10^5$; $5 - 4\times10^5$ W/cm^2; EHD—emission band of electron-hole drops. b) Dependence of the EHD emission intensity on the excitation level. c) Dependence of the EHD band intensity and of the line of the exciton bound on the S impurity on the delay time relative to the excitation pulse.

of the maximum up to ~2.28 eV likewise remained unchanged. With further increase of W to $\sim4\times10^5$ W/cm^2 the band as a whole was shifted by approximately 4 meV towards higher energies. The EHD band competed with the recombination of excitations bound on the donor S, and were observed only in the purest samples (see Ref. 19), in which

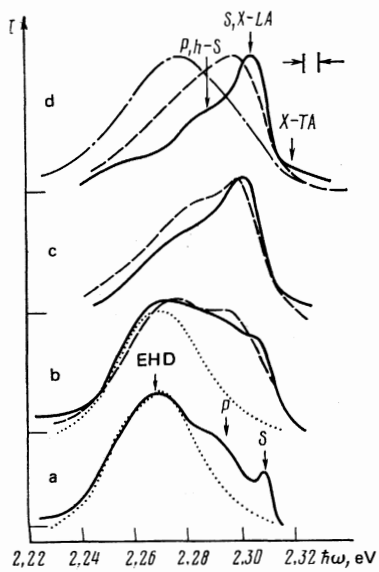

FIG. 2. Variation of GaP emission spectra with temperature T: a—30, b—39, c—46, d—60 K; excitation density: solid—2×10^4, dashed—1×10^5, dash-dot—4×10^5 W/cm^2. Next to curves a and b are shown dotted the theoretical curves obtained from (8) with parameters from Tables I and II.

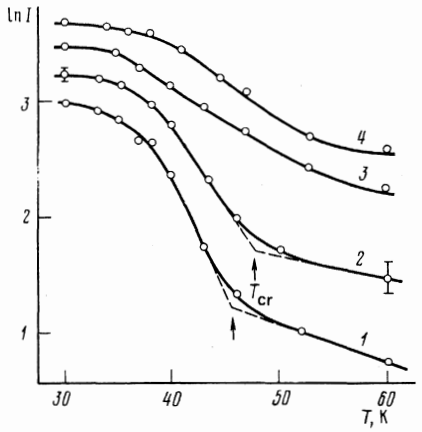

FIG. 3. Temperature dependence of the emission intensity at the maximum of the EHD band at different excitation densities W: $1 - 2\times10^4$; $2 - 10^5$; $3 - 2\times10^5$; $4 - 4\times10^5$ W/cm^2.

the S line was weaker by a factor 5–10 than in the remaining ones. It appears that in these five samples the donor density reached $< 10^{16}$ cm^{-3}.

In the short-wave part of the band at energies $\hbar\omega > 2.28$ eV, the spectrum changed when the excitation level was increased. Thus, the ratio of the luminescence intensity near the shoulder at $\hbar\omega_P = 2.295$ eV to the intensity near the maximum, $\hbar\omega_m$(EHD) = 2.268 eV, changed from 0.56 to 0.42 when W was increased from 5×10^3 to 2×10^5 W/cm^2. This is evidence that the shoulder in the short-wave part of the band is due to a recombination mechanism other than EHD, which was attributed in earlier papers[10,11] to recombination in a low-density electron and hole plasma (the arrow P in Fig. 1).

The dependence of the PL intensity at the maximum of the EHD band on W is shown in Fig. 1b. The plot shows a characteristic kink at $W_{cr} = 3\times10^3$ W/cm^2. At lower W, the plot is approximately linear, and at higher it follows a power law with exponent 2.2 ± 0.2. At the highest excitation densities the $I(W)$ dependence becomes weaker than quadratic.

The dependence of the emission intensity on the delay time τ relative the excitation pulse is shown in Fig. 2c. Near $\tau = 20$ nsec a maximum of I(EHD) is observed, after which the intensity decreases exponentially with a lifetime τ(EHD) = 30 ± 3 nsec. The intensity of the S line reached a maximum at $\tau = 50$ nsec, and the characteristic falloff time was ~150 nsec.

3.2. When the temperature was raised to ~40 K the spectra had similar dependences on W and τ (Figs. 2a, 2b). In the interval $T = 40$–50 K the spectra underwent substantial changes. At $W = 2\times10^4$ W/cm^2 the broad band corresponding to the EHD vanished. Lines of a free excitation with emission of *TA*, *LA*, and *TO* phonons appeared in the short-wave part of the spectrum and were most strongly pronounced at $T = 60$ K. In addition, a hole–donor line (*h–S*) appeared. The intensity ratio of the phonon replicas in the excitation spectra could not be determined because of the influence of the *h–S* bands.

When W was increased to 10^5 W/cm^2 it became possi-

ble to distinguish a P band in the spectrum. At the highest densities, $W \gtrsim 4\times10^5$ W/cm^2, the broad band with maximum $\sim$2.28 eV did not vanish from the spectra up to $\sim$60 K (dash-dot line in Fig. 2d). The spectral position of this band was close to the EHD band. At such W, however, the luminescence spectra changed and differed from the EHD band even at low T. The interpretation of this band is not unique, and the discussion that follows is confined to the results obtained at $W \leqslant 2\times10^5$ W/cm^2.

For a more accurate determination of the critical temperature in the 40–50 K interval we investigated the dependence of the PL intensity at the maximum of the EHD band, I_m (EHD), on T (Fig. 3). A distinguishing feature is the rapid decrease in the interval 40–50 K and the slower decrease at $T \gtrsim 50$ K. If the critical temperature is chosen to be the point of transition from the rapid to the slow decreaes, we get $T_c = 48 \pm 2$ K. If the possible difference between the crystal and substrate temperatures is taken into account, the critical temperature for the EHD in GaP must be taken to be $T_c = 50^{+5}_{-3}$ K.

Thus, the shape of the emission spectra, the critical dependence on the excitation level and on the temperature, the short characteristic luminesence falloff time indicate that electron-hole drops were observed in our experiments. They agree with the experimental data[10,11] and provide a more accurate value of T_c.

4. ANALYSIS OF THE SHAPE OF THE EHD SPECTRA AND DISCUSSION OF RESULTS

4.1. Figure 4 shows the electronic-transition scheme for strong degeneracy and for equal electron and hole densities,

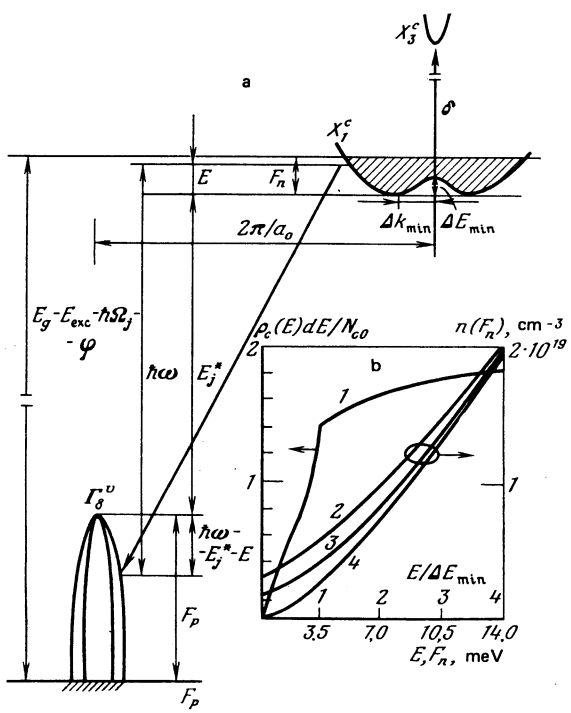

FIG. 4. a) Scheme of radiative electronic transitions in EHD in GaP. b) Dependence of the state density on the energy (curve 1) and of the electron density on the Fermi quasilevel (curves 2–4) at various temperatures (2–50, 3–40, 4–8 K), calculated from Eqs. (2) and (3).

TABLE I. Gallium-phosphide parameters used in the calculation of the emission spectra.

Parameter	Value	Reference
E_g(4,2K)	2.350 eV	[14, 15]
E_g(50K)	2.347 eV	–
E_{exc}	21 meV	[16]
$\hbar\Omega(TA)$	13.2 meV	[5]
$\hbar\Omega(LA)$	32.2 meV	–
$\hbar\Omega(TO)$	46.4 meV	–
$I_{TO} : I_{LA} : I_{TA}$	0.40 : 1 : 0.34 (1) 0.25 : 1 : 0.38 (2)	[10] [5]
δ	0.354 eV	–
D^*	1.22±0.01	[14–16]
ΔE_{min}	3.5±0.3 meV	–
$m^*_{c\parallel}/m_0$	0.9	–
$m^*_{c\perp}/m_0$	0.254	[5]
$(m^{*3/2}_{vh} + m^{*3/2}_{vl})^{2/3}/m_0$	0.626 0.541	[20] [10]
N_{c0}	$3.46\cdot10^{18}$ cm^{-3}	–

$n = p$. Account is taken for the two-hump structure of the conduction band, with a distance δ between the spectrum branches X_1^c and X_3^c. The "hump" ΔE_{min} is given by

$$\Delta E_{min} = \delta (D^*-1)^2/4D^*, \tag{1}$$

where $D^* = (2m_0/\hbar^2)(D^2/\delta)$ is the parameter of the $\mathbf{k}\cdot\mathbf{p}$ interaction. The state density $\rho(E)dE$ in this structure was calculated in Refs. 10–16. It is convenient to write it in the form

$$\rho_c(E)\,dE = N_{c0}\,d\varepsilon \begin{cases} [1+(\varepsilon-1)(D^*-1)/2D^*+\varepsilon^{1/2}]^{1/2} \\ -[1+(\varepsilon-1)(D^*-1)/2D^*-\varepsilon^{1/2}]^{1/2}, & \varepsilon<1, \\ [1+(\varepsilon-1)(D^*-1)/2D^*+\varepsilon^{1/2}]^{1/2}, & \varepsilon\geqslant 1, \end{cases} \tag{2}$$

where the energy is reckoned from the bottom of the band, and the height of the hump is set equal to unity, $\varepsilon = E/\Delta E_{min}$. The parameter N_{c0} is determined by the effective masses m_c^* and $m_{c\parallel}^*$ and by the parameters D^*, δ, and ΔE_{min}:

$$N_{c0} = \frac{3}{2\pi^2}\left(\frac{2m_0}{\hbar^2}\right)^{3/2} \frac{m^*_{c\perp}}{m_0}\left(\frac{m^*_{c\parallel}}{m_0}\right)^{1/2}\left(\frac{\delta}{2}\right)^{3/2}\frac{(D^*-1)^{5/2}}{2D^*}.$$

In contrast to Refs. 10 and 11, we regard the numerical values of the parameters to be not as obtained by fitting, but as known from Refs. 14–16 (Table I).

The conduction band is asymmetric and highly nonparabolic; the function $\rho_c(E)$ calculated from Eq. (2) is shown in Fig. 4. The same figure shows the dependence of the electron density

$$n = \int_0^\infty \rho_c(E) f_c(E, F_n)\,dE, \qquad f_c = \left[1+\exp\frac{E-F_n}{kT}\right]^{-1} \tag{3}$$

on the Fermi quasilevel F_n. The calculations lead to a convenient approximation in the density interval $n = (0.7$–$2)\times10^{19}$ cm^{-3}:

$$n = N_{c0}k(F_n/E_{min})^\nu, \tag{4}$$

where the coefficient k and the exponent ν vary little in the interval $T = 0$–40 K, namely $k = 0.91$–1.22 and $\nu = 1.31$–1.14.

At sufficiently large $F_n \gtrsim 6$ meV the average electron kinetic energy increases thus with the density faster than $\sim n^{3/2}$; under this condition a better assumption is that the many-electron effects influence little dispersion in the EHD. We note that at smaller F_n the kinetic energy increases more

slowly than $\sim n^{2/3}$ and the question of the influence of many-electron effects on the dispersion law remains open.

From (4) and from the parabolic approximation of the dispersion in the valence band:

$$\rho_v(E') = {}^1/_2\pi^{-2}[2(m_{vh}^{*3/2} + m_{vl}^{*3/2})^{2/3}/\hbar^2]^{3/2}E'^{1/2} \quad (5)$$

with effective masses m_{vh}^* and m_{vl}^* of the heavy and light holes, given in Table 1 of Ref. 20, follows an approximation for the Fermi quasilevel F_p at $n = p$:

$$F_p = (3.92-6.02)F_n^{(0.87-0.76)}, \quad T=0-40\ \text{K} \quad (5^*)$$
(F_p and F_n in meV).

At the typical densities $\sim 10^{19}\ \text{cm}^{-3}$ the carriers occupy a rather large part of the Brillouin zone along axes of the (100) type:

$$\Delta k = \Delta k_c + \Delta k_v \approx (0.17+0.06)(2\pi/a_0), \quad (6)$$

where $a_0 = 5.449$ Å for GaP (Refs. 4 and 5). Figure 4 illustrates the calculations by formulas (2)–(6) for values $n = p \approx 10^{19}\ \text{cm}^{-3}$.

Note that we have chosen larger hole effective masses than in Ref. 10 (Table I). It is known that the effective hole masses increase with density p if the latter is increased on account of an increase in the acceptor density N_A (Ref. 5). There are no published data on m_{vh}^* and m_{vl}^* in GaP with small N_A at large equilibrium values of p.

4.2. We calculate now the EHD emission spectra, following Refs. 9–11 and taking into account the described peculiarities of the GaP band structure. It is assumed in the calculation that the many-electron interaction shifts the spectrum as a whole, but does not change the shapes of equal-energy surfaces in the EHD, i.e., we can neglect the damping of the Bloch waves and the renormalization of the effective mass. This assumption holds for Ge and Si with accuracy 10–15%. According to estimates,[10,21] the EHD binding energy in GaP is $\varphi \approx 12$–17 meV; this is noticeably larger than the parameter $\Delta E_{\min}$ (Table I). It is therefore not obvious beforehand that the exchange, correlation,[2] and electron-phonon[22] interactions do not distort the spectrum near the edge of the two-hump structure. If the assumption is correct for GaP, the width of the forbidden band in the EHD is

$$E_g^* = E_g - (E_{exc}+\varphi) - (F_n+F_p), \quad (7)$$

where E_{exc} is the free-excitation ionization energy (Table I).

It is assumed that the probabilities of emission of various phonons for indirect transitions in EHD remain the same as for free excitons. However, owing to the condition (6), the situation in GaP differs from Ge and Si: The energies of the emitted phonons can differ, in accord with their dispersion near the points X and Γ (see Ref. 5) from the values at the point X listed in Table I. The difference from the estimated Δk amounts to $\Delta\hbar\Omega_{LA} \approx 3$ meV and $\Delta\hbar\Omega_{TO,LA} \approx 0.5$ meV.

It is assumed that the effective electron and hole temperature equals the lattice temperature. This assumption calls for verification, since the carrier lifetimes in GaP are substantially shorter than in Ge and Si, although they remain much longer than the relaxation times in the bands.

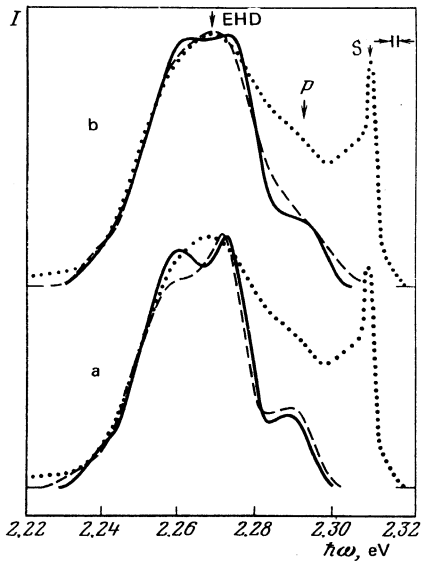

FIG. 5. Comparison of the experimental emission spectrum at $T = 8$ K (points) with the theoretical calculation of the EHD of the spectra of EHD in GaP; a—the solid and dashed curves correspond to sets 1 and 2 of Table I; b—solid curve—set 1, $T = 30$ K, dashed—calculated from Eq. (9) with $\sigma = 3$ meV.

With these stipulations, we write down the equation for the emission spectrum:

$$I(\hbar\omega) \sim \sum I_j \iint dE\,dE'\rho_c(E)\rho_v(E')f_c(E,F_n) \times [1-f_v(E',F_p)]\delta[\hbar\omega-(E_g^*-\hbar\Omega_j+E+E')]. \quad (8)$$

Using the energy conservation law in the form of a δ function and putting $E_j^* = E_g^* - \hbar\Omega_j$ we obtain

$$I(\hbar\omega) \sim \sum_j I_j \int_0^{\hbar\omega-E_j^*} dE\rho_c(E)\rho_v(\hbar\omega-E_j^*-E)f_c(1-f_v), \quad (8')$$

where the summation is over the three phonons $j = TO, LA$, and TA (Table I). Different phonon emission probabilities I_j obtained from exciton luminescence are cited by different workers, in view of the presence, in the experimental spectra, of bands produced by various recombination mechanisms and obscuring the true I_j. Table I lists two sets of I_j (1 and 2).

4.3. The results of computer calculations in accord with Eq. (8′) are shown in Fig. 5 and are compared with the experimental data at $T = 8$ K. In the calculations we varied the quasilevels F_n and F_p and used Eqs. (4)–(6). The values of φ were chosen by shifting the calculated curve relative to the experimental one. Figure 5a shows the difference for the different sets of phonon-emission probabilities: At large I_{TO}/I_{LA} the theoretical spectra acquire a structure not observed in either our experiments or in Refs. 10 and 11. The experimental spectra have a flatter peak than the calculated ones.

Better agreement with experiment is obtained if an electron temperature $T = 30$ K is assumed at the same values of n_0, as shown by the dashed curve in Fig. 5b. An attempt was also made to describe phenomenologically the experimental spectrum with allowance for the possible smearing of the spectra on account of violation of the assumptions discussed

TABLE II. Experimental parameters of EHD in GaP and their comparison with the calculations. The value of φ was determined by a best fit either to the maxima (*) or to the long-wave edges (**) of the spectra for two sets of phonon-emission probabilities (1 and 2).

T_c, K	F_n, meV	F_p, meV	n_0, 10^{19} cm^{-3}	φ, meV		Reference
				*	**	
$50\ ^{+5}_{-3}$	10±0.5	32±2	1.2±0.2	15 18	19 (1) 21 (2)	Present work
45	5.4	26.6	0.86	17.5±3		[10]
70	13.3	26.7	0.74	15		[11]

in Sec. 4.2. To this end the δ function in the integral of (8) was replaced by the Gaussian $\Psi(\hbar\omega - E,\sigma)$ with a scatter parameter σ equal to the estimated value of $\Delta\hbar\Omega_{LA}$:

$$I(\hbar\omega) = \int dE\,\Psi(\hbar\omega - E,\sigma)\,I(E),$$
$$\Psi(\hbar\omega - E,\sigma) = \frac{1}{(2\pi)^{1/2}\sigma}\exp\left[-\frac{(\hbar\omega - E)^2}{2\sigma^2}\right]. \quad (9)$$

Numerical integration using Eq. (9) at $\sigma = 3$ meV and the function $I(E)$ calculated from (8′) has shown that the calculated shape of the spectra agrees better with experiment (solid curve in Fig. 5b).

Owing to the difference between the experimental and theoretical spectra, the fit of the parameters F_n, F_p, and φ to Eq. (8) depended on the manner of fitting—on whether the best agreement was obtained in the long-wave part or in the region of the band maximum. The results are given in Table II, which lists also data from Refs. 10 and 11. Our analysis shows that the parameters in Refs. 10 and 11 were chosen with exaggerated accuracy. Allowance for phonon dispersion or for the smearing of the spectrum as a result of many-electron interaction should lead, as shown by estimates using (9), to a decrease of the chosen value of the sum $F_n + F_p$ and to a corresponding decrease of the carrier density in the EHD. A decreae of the relative *TO*- and *TA*-phonon emission probabilities introduced into the calculations should increase the chosen values of F_n and F_p and accordingly of n_0.

A more accurate comparison of the experimental data with the theory is as yet meaningless, since account must be taken of the factors that restrict the use of Eq. (8). The order of magnitude of the correction is estimated to be the value of σ in (9). One of the factors that must apparently be taken into account is that the electrons and holes in the EHD have a higher temperature than the lattice.

4.4. If the parameters n_0 and φ determined from experiments at low T are used to calculate the spectra at higher temperatures, it becomes obvious that other recombination mechanisms affect the spectra (see Figs. 2a and 2b). The plasma emission (P) prevails over the EHD emission at $T \gtrsim 40$ K, and the EHD role can be tracked only to ~ 48 K. It was therefore impossible to estimate the change of the EHD parameters with increasing T from a comparison of the calculations with experiment. We note that the recombination mechanism that determines the P band is not yet clearly understood.

5. CONCLUSION AND DEDUCTIONS

1. Radiation due to electron-hole drops is observed in epitaxial GaP films with impurity density $\lesssim 10^{16}$ cm^{-3} at $T = 8$–50 K. The emission spectra can serve as a measure of the purity of the GaP crystals.

2. In the excitation-level interval $W = 3\times10^3$–2×10^5 W/cm^2 at temperatures $T \lesssim 40$ K the shape of the EHD band with the maximum $\hbar\omega_m = 2.268$ eV does not depend on W and T. The band has characteristic recombination times $\tau = 30 \pm 3$ nsec and a critical temperature $T_c = 50\ ^{+5}_{-3}$K.

3. To determine the EHD parameters by comparing the experiments with the theoretical calculation it is necessary to choose correctly the parameters of the two-hump structure of the conduction band and the ratio of the phonon emission probabilities in indirect transitions. The analytically obtained Fermi quasilevel values $F_n = 10 \pm 0.5$ meV and $F_p = 32 \pm 2$ meV, density $n_0 = 1.2\times10^{19}$ cm^{-3} in the EHD, and binding energy $\varphi = 19 \pm 2$ meV must be refined to allow for the phonon dispersion and for heating of the carriers in the EHD.

4. At quantum energies ~ 2.29 eV, near the short-wave edge of the EHD band at high T, an important role is assumed by a recombination band assumed to be due to a low-density electron-hole plasma.

The authors are deeply grateful to O. B. Nevskiĭ for supplying the samples, to A. N. Nikhtin and A. A. Kopylov for a helpful discussion of questions connected with the two-hump structure of the conduction band, and to É. Yu. Barinova and M. V. Chukichev for help with the work.

[1]Ya. E. Pokrovski, Phys. Stat. Sol. (a) **11**, 385 (1972).
[2]T. Rice, J. Hensel, T. Philips, and G. Thomas, Electron-Hole Liquid in Semiconductors [Russ. transl.], Mir, 1890.
[3]A. A. Bogachev, Prog. Quant. Electron. **6**, 141 (1980).
[4]A. A. Bergh and P. J. Dean, Clarendon Press, 1976.
[5]A. E. Yunovich, Fortschr. Phys. **23**, 317 (1975).
[6]J. Shah, R. F. Leheny, W. R. Harding, and D. R. Wight, Phys. Rev. Lett. **18**, 1164 (1977).
[7]H. Maaref, J. Barrau, M. Brousseau, J. Collet, and J. Mazaschi, Sol. St. Commun. **22**, 599 (1977); **25**, 601 (1978).
[8]D. Hulin, M. Combescot, N. Bontemp, and A. Mysyrovicz, Phys. Lett. **61A**, 349 (1977).
[9]C. Benoit á la Gillaume, N. Bontemps, D. Hulin, and A. Mysyrowicz, J. Lumin. **18/19**, 532 (1979).
[10]D. Bimberg, M. S. Skolnik, and L. M. Sander, Sol. St. Commun. **27**, 949 (1978); Phys. Rev. **B 19**, 2231 (1979).
[11]R. Schwabe, F. Thuselt, H. Weinert, R. Bindemann, and K. Unger, Phys. Stat. Sol. (b) **89**, 561 (1978).
[12]M. Capizzi, F. Evangelisti, A. Prova, and F. Pantella, Sol. St. Commun. **24**, 801 (1977).
[13]M. Altarelli, R. A. Sabatini, and N. O. Lipari, Sol. St. Commun. **25**, 1101 (1978).
[14]A. A. Kopylov and A. N. Pikhtin, Fiz. Tekh. Poluprov. **11**, 867 (1977) [Sov. Phys. Semicond. **11**, 510 (1977)].

[15]A. N. Pikhtin and A. A. Kopylov, Sol. St. Commun. **26**, 735 (1977).
[16]G. F. Glinskiĭ, A. A. Kopylov, and A. N. Pikhtin, Fiz. Tekh. Poluprov. **12**, 1327 (1978) [Sov. Phys. Semicond. **12**, 737 (1978)].
[17]V. A. Fedorov, O. B. Nevskiĭ, O. I. Kravchenko *et al.*, Dokl. Akad. Nauk SSSR **253**, 428 (1980).
[18]M. S. Minazdinov, O. B. Fedorov, and O. B. Nevskiĭ, Elektron. Prom. Nos. 8(92)–9(93), 60 (1980).
[19]N. R. Nurtdinov, M. V. Chukichev, and A. E. Yunovich, Abstracts, All-Union Conf. on Phys. of III–V Compounds, Novosibirsk, 1981, p. 143.
[20]J. Leotin, R. Barbaste, S. Askenary *et al.* Sol. St. Commun. **15**, 693 (1974).
[21]R. K. Kalia and P. Vashishta, Sol. St. Commun. **34**, 121 (1980).
[22]L. V. Keldysh and A. P. Silin, Zh. Eksp. Teor. Fiz. **69**, 1053 (1975) [Sov. Phys. JETP **42**, 535 (1975)].

Translated by J. G. Adashko